Seismic imaging of the 1999 Izmit (Turkey) Rupture inferred from the near-fault recordings

Michel Bouchon, Nafi Toksöz, Hayrullah Karabulut, Marie-Paule Bouin, Michel Dietrich, Mustafa Aktar, Margaret Edie

GEOPHYSICAL RESEARCH LETTERS, VOL. 27, NO. 18, PAGES 3013-3016, SEPTEMBER 15, 2000

Seismic Imaging of the 1999 Izmit (Turkey) Rupture Inferred from the Near-Fault Recordings

Michel Bouchon,[1] Nafi Toksöz,[2] Hayrullah Karabulut,[3] Marie-Paule Bouin,[4]
Michel Dietrich,[1] Mustafa Aktar,[3,5] and Margaret Edie[2]

Abstract.
We use near-fault accelerograms to infer the space-time history of rupture on the fault during the Izmit earthquake. The records show that the ground displacement and velocity near the fault were surprisingly simple. Rupture propagated toward the west at a velocity of about 3 km/s, and toward the east at a remarkably high average velocity of 4.7 km/s over a distance of about 45 km before decelerating to about 3.1 km/s on the eastern segment. Slip on the fault is particularly large down to a depth of 20 km on the central portion of the fault where it reaches about 7 m. Slip is large also below 10 km on the eastern fault segment, and this may have contributed to the loading of shear stress on the Düzce fault. On the western fault segment, large slip seems confined to shallow depths.

Introduction

The Izmit earthquake of August 17 1999 broke a long segment of the North Anatolian fault zone. Its surface rupture runs nearly east-west and extends over at least 120 km. Surface slip is almost pure right-lateral strike-slip and ranges, over most of the surface break, between 1.5 m and 5 m [*Toksöz et al.*, 1999].

Ground motion near the fault

Six accelerometer stations installed and operated by Boğaziçi University and by the General Directorate of Disaster Affairs recorded the earthquake ground motion at close distance from the fault. We shall use in this study the records obtained at four of these stations, which are displayed in Figures 1 and 2. They are records of the ground velocity and are obtained by integrating the accelerograms. The four corresponding stations (ARC, IZT, SKR, DZC) are distributed rather uniformly along the line of rupture (Figure 3a). Of the two stations that we did not use, one (GBZ) is located very close to ARC, and the ground velocities there display waveforms and amplitudes similar to those at ARC. The digital records at ARC are, however, of much better quality than the analog records at GBZ, and, for this reason, we shall use ARC as our modeling station. The other station that we did not use is YPT because records there are more complicated and have a longer duration than records at ARC and SKR, located further from the epicenter. This complexity suggests that at this station the records are more affected by the shallow crustal structure below the site or between the station and the fault.

Ground velocity at the westernmost site (ARC), located 50 km from the epicenter and about 10 km from

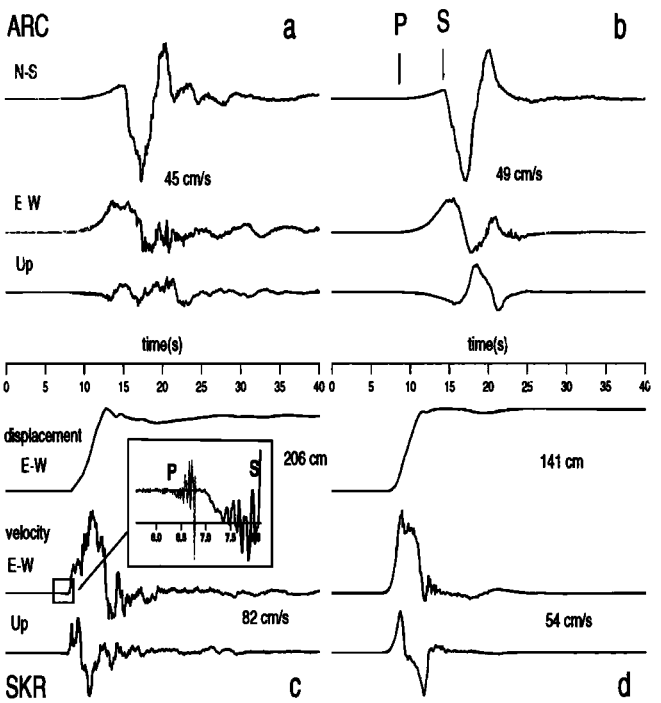

Figure 1. (a) Ground velocity recorded at ARC and (b) calculated for a rupture velocity of 3 km/s and a fault slip and geometry based on surface observations. (c) Displacement and velocity recorded at SKR and (d) calculated for a rupture velocity of 4.7 km/s. The values indicated are the peak amplitudes of the observed/calculated velocity/displacement. All the traces start at the origin time of the rupture which is inferred from the hypocentral P wave travel time. The zoom in (c) presents the P and S arrivals on the vertical accelerogram and the horizontal velocity record respectively.

[1]Université Joseph Fourier, Grenoble, France
[2]Massachusetts Institute of Technology, Cambridge, Massachusetts
[3]Boğaziçi University, Kandilli Observatory, Istanbul
[4]Institut de Physique du Globe, Paris
[5]Tübitak, Marmara Research Center, Gebze, Turkey

Paper number 2000GL011761.
0094-8276/00/2000GL011761$05.00

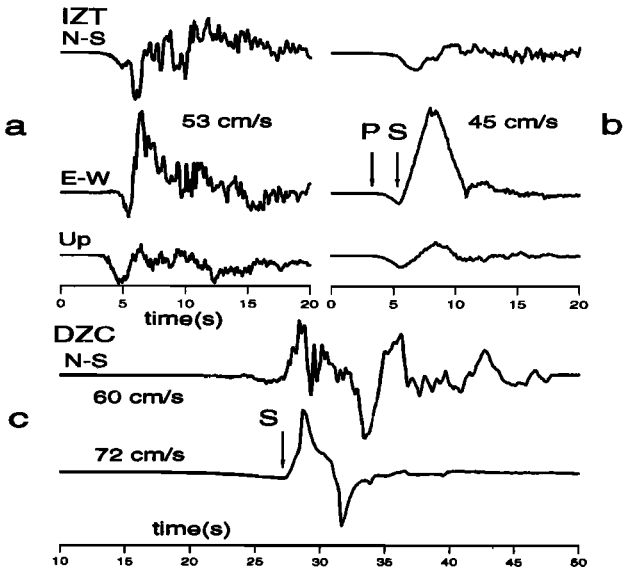

Figure 2. (a) Ground velocity recorded at IZT and (b) calculated for a rupture velocity of 3 km/s and a fault slip and geometry based on surface observations. (c) N-S ground velocity recorded (top) and calculated (bottom) at DZC. The traces start at the origin time of the rupture except the DZC record for which the absolute time is not known. The values indicated are the peak amplitudes of the observed/calculated velocity.

the fault, are displayed in Figure 1a. The records there are surprisingly simple. The largest motion is transverse to the fault (N-S) with the peak amplitude of the pulse directed toward the south. This is what is expected at this location for a right-lateral strike-slip fault propagating westward toward the station, based on previous experience [1966 Parkfield (*Aki,* 1968); 1979 Coyote Lake (*Bouchon,* 1982); 1979 Imperial Valley (*Archuleta,* 1982)]. The simplicity of the transverse pulse, made-up mostly of SH-waves, indicates that the propagation of the waves, from the fault to the station, was not significantly affected by near-surface sediments which would otherwise have produced a more complex waveform.

In order to further understand these records, we model the earthquake as a rupture which starts at the hypocenter and propagates radially on the fault. The fault geometry considered is made-up of several segments which follow the surface breaks and are vertically dipping from the surface to 20 km (Figure 3a). Slip is assumed to be horizontal and constant with depth but varies along the fault strike according to the values measured at the surface. The upper crust is chosen to be uniform with P and S wave velocities of 6 km/s and 3.46 km/s, respectively. Below 16 km, these velocities increase to 6.3 km/s and 3.64 km/s. The crust is 32 km thick and P and S velocities below the Moho are 8 km/s and 4.6 km/s, respectively. The rupture velocity is uniform and equal to 3 km/s. Slip on the fault is assumed to grow as a ramp function starting at the arrival of the rupture front and stopping 3 s later. The calculation is performed using the discrete wavenumber method [*Bouchon,* 1981] where the fault is represented by 10800 point double-couple sources distributed on the fault surface at 500 m spacing.

The results of the calculation are shown in Figure 1b. The calculated ground velocity explains remarkably well the one which took place during the earthquake. The N-S motion starts with the arrival of the P-wave, which in the near-field displays a component of motion transverse to the traveling direction. The motion is reversed at the arrival of the S-wave and the maximum of the pulse corresponds to the passage of the rupture front close to the station. As expected the first motion is down and toward the east, but the presence of a transverse component to the P wave adds a slight northerly motion. A second integration of the velocity records, not shown here, yields a static displacement of the station of 51 cm in the N105°E direction.

The ground velocity at SKR is displayed in Figure 1c. At this station, located 34 km due east of the epicenter, the N-S component was not working. The other records there are, however, most remarkable, the double integration of the E-W acceleration (upper trace in Figure 1c) yielding a simple displacement waveform dominated by a static displacement of the station of 2 m toward the east. The timing of the P and S wave arrivals at SKR can be seen on the enlarged picture of the beginning of the E-W velocity record displayed in Figure 1c. Also shown on this picture is the arrival of the P wave on the vertical accelerogram, where it is the easiest to identify. The measured S minus P time of about 1.8 s is much shorter than the one expected (about 4.5 s) for an hypocentral distance of 38 km. As shown by *Ellsworth and Celebi* [1999], this implies that the rupture propagated at a supershear velocity between the hypocenter and SKR and yields an average rupture velocity of 4.7 km/s on this part of the fault. These records provide the first direct measurement of a supershear rupture velocity. They confirm previous indirect inferrences of supershear velocity made most notably by *Archuleta* [1984] for the 1979 Imperial Valley earthquake. The good agreement of the recorded waveforms with the ones calculated for the fault model previously described and a rupture velocity of 4.7 km/s (Figure 1d) confirms the high value obtained. Simulations made with sub-shear or shear rupture velocities show a slow amplitude build-up of the E-W and vertical pulses between the P and S arrivals, similar to the ones observed at ARC, inconsistent with the sharp beginning of the observed pulses.

Ground acceleration at the other two stations (IZT and DZC) were triggered analog recordings. For this reason, the quality of the records is not as good as at SKR and ARC and the integration process is less stable. These recordings nevertheless provide important information on the rupture history of the earthquake. The one at IZT (Figure 2a) is obtained only a few kilometers away from the epicenter. The first motion is a dilatation, indicating that the epicenter lies

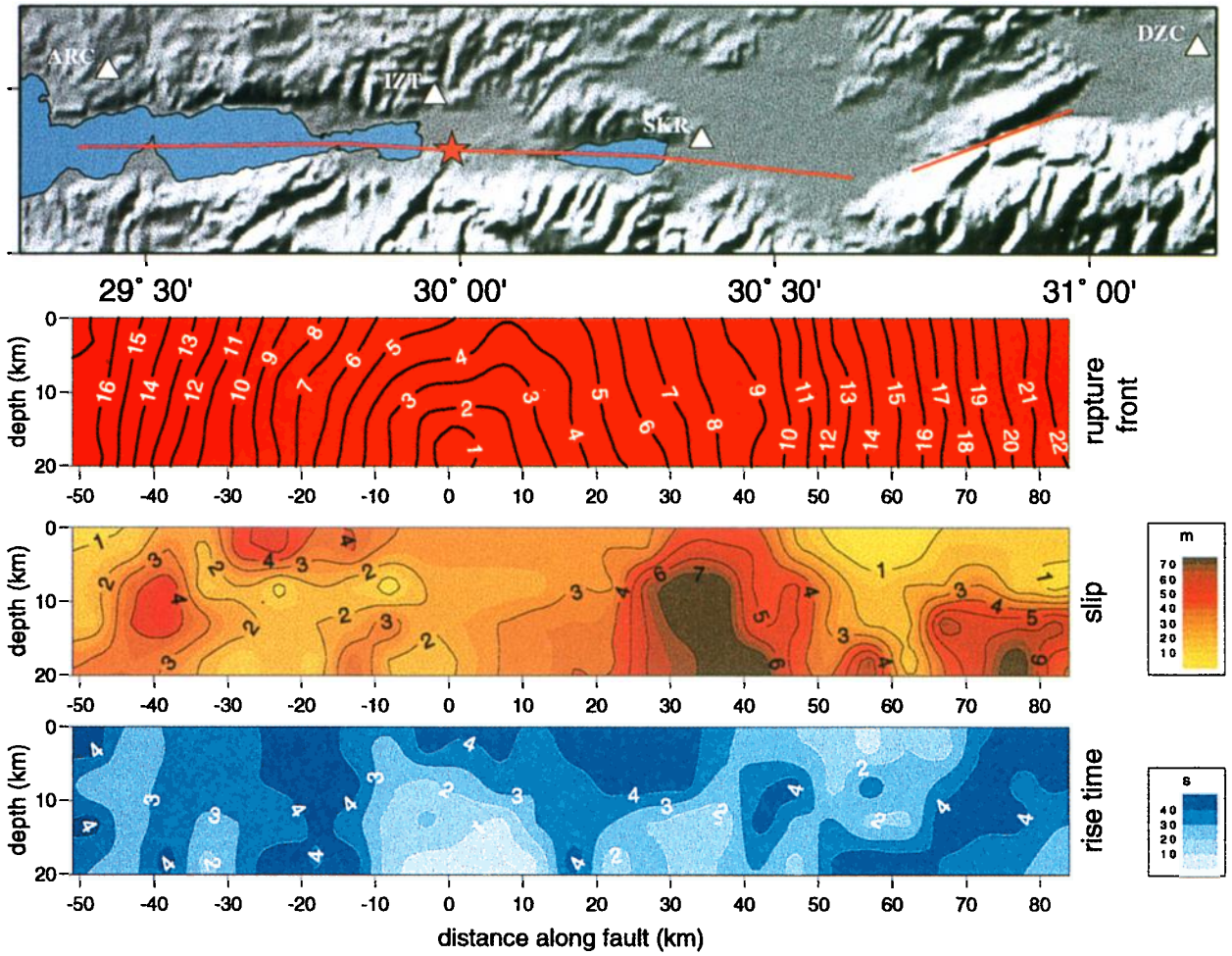

Figure 3. (a: Top) Map of the surface rupture of the Izmit earthquake (red line). The star indicates the location of the epicenter and the triangles are the recording stations. (b: Middle and bottom) Images of the rupture front, slip, and rise time on the fault. The rupture front is shown at 1 s intervals from the beginning of rupture.

slightly east of the station. The S wave arrives 2.3 s after the beginning of the record which, if one assumes that the instrument was triggered by the first ground vibration, yields an hypocentral depth of 17 km. This station thus confirms with precision the location of the epicenter and the depth of nucleation. It also shows that rupture propagated upward from the hypocenter at an average velocity not exceeding the crustal shear wave velocity. The ground velocity calculated with the previously-described fault model and a rupture velocity of 3 km/s (Figure 2b) provides a reasonably good fit to the first few seconds of motion, except that the time build-up of the calculated pulses is less steep than the observed one. This suggests that the slip rise time in the hypocentral area was shorter than the 3 s used in the simulation.

The ground accelerations at DZC were also analog records. Furthermore, the large epicentral distance of the station, 100 km (Figure 3a), does not insure that the instrument was triggered by the first P arrival. Nevertheless these records also provide useful information on the rupture history of the earthquake. Because of the station location, about 20 km beyond the eastern end of the surface rupture, the N-S ground motion, more transverse to the fault, is expected to be dominant there and to be the easiest one to interpret in terms of fault rupture. This N-S ground velocity is displayed in Figure 2c. A comparison with the calculation done with a rupture velocity of 4 km/s is also shown and allows the clear identification of the S arrival. With the uncertainty on the triggering time, its timing is not precisely known. The earliest possibility (23.4 s) is obtained when assuming that the instrument triggered on the first arrival. The latest one (27.6 s) is inferred by adding to the S arrival time at SKR, the shear wave travel time between SKR and DZC. The true S arrival time lies between these two values. The time span between the northern and southern velocity peaks carries information on the apparent duration of fault rupturing as seen from DZC. The average rupture velocity of 4 km/s used in the model clearly underestimates this duration.

Seismic imaging of the rupture

In order to infer in more details the space and time history of the rupture, one needs to apply some inver-

sion scheme to the data. We shall use here a scheme based on simulated annealing to sample the space of possible model parameters and to determine, in this space, the set of parameters which best fit the ground velocities recorded at ARC, IZT, SKR, and DZC. The method of simulated annealing has been used quite successfully by previous authors to infer the source characteristics of earthquakes [*Hartzell and Liu*, 1995; *Courboulex et al.*, 1996; *Ihmlé*, 1996] and we refer to these studies for a description of the algorithm.

The fault geometry was shown in Figure 3a. The fault is discretized into 108 sub-elements of 5x5 km, each element being represented by 25 double-couple point sources. The slip, rise time, and rupture velocity of each element constitute the space of model parameters. At first, this space is uniformly sampled. Causality of the rupture is required, implying that the rupture front cannot reach a sub-element before having reached the one below it and the neighboring one closer to the epicenter. Slip in all the uppermost fault elements located on land is set at the value measured at the surface. Elsewhere slip is allowed to vary between 0 and 8 m. Rise time may vary between 0.25 s and 5 s. Average rupture velocities on the westward, central, and eastern fault segments are allowed to vary between 2 and 6 km/s. Local rupture time occurs within a 1 s time window centered on the average rupture velocity. Because the absolute time is not known at DZC, the S wave arrival time there is allowed to vary uniformly in the range of possible values previously discussed. The best fit is determined by the minimization of the cost function:

$$S = \sum_{j=1}^{4} \sum_{i=1}^{N} [C_j(i) - O_j(i)]^2 \qquad (1)$$

where $C_j(i)$ and $O_j(i)$ are respectively the calculated and observed ground velocities at station j and time i. N is taken equal to 64 points representing 30 s of signal except at IZT where the first 12 s of signal only are considered. No filtering is applied to the data.

The results obtained are presented in Figure 3b. Successive positions of the rupture front, displayed at 1 s intervals, show the supershear propagation of rupture over about 45 km of the fault. Beyond this distance, rupture decelerates to about 3.1 km/s. The westward propagation of rupture from the hypocenter takes place at an average rupture velocity of 3 km/s. The largest slip occurs between 25 and 45 km east of the epicenter where it reaches about 7 m. Slip is large also below 10 km on the eastern fault segment (about 5 m), and this may have contibuted to the loading of shear stress on the Düzce fault. West of the epicenter, slip is large between distances of 10 and 30 km, which is the region around Gölcük, the hardest hit area during the earthquake. There, large slip of about 4 to 5 m is confined to shallow depths. The rise time which represents the duration of slipping locally on the fault is generally of the order of 2 to 4 s, except in the hypocentral area where it is the shortest (about 1 s).

Acknowledgments. We are most thankful to the scientists, engineers, and technicians at Boğaziçi University in Istanbul and at the General Directorate of Disaster Affairs in Ankara who are in charge of the strong motion stations whose recordings are the basis of the present study. We thank Mustafa Erdik, Cécile Cornou, Robert Guiguet, Aybige Akinci, Henri Haessler, Rolando Armijo, Cemil Gürbüz, Sadi Kueli, Gündüz Horasan, Armando Cisternas, Bertrand Meyer, Jean-Bernard de Chabalier, Pierre-Yves Bard, and Jean-Robert Grasso for their help and discussions in the course of this work. We also thank Jiri Zahradnik for his comments. This study was partly financed by CNRS and ANDRA through the GdR FORPRO.

References

Aki, K., Seismic displacement near a fault, *J. Geophys. Res., 73,* 5359-5376, 1968.

Archuleta, R.J., Analysis of near-source static and dynamic measurements from the 1979 Imperial Valley earthquake, *Bull. Seismol. Soc. Am., 72,* 1927-1956, 1982.

Archuleta, R.J., A faulting model for the 1979 Imperial Valley earthquake, *J. Geophys. Res., 89,* 4559-4585, 1984.

Bouchon, M., A simple method to calculate Green's functions in elastic layered media, *Bull. Seism. Soc. Am., 71,* 959-971, 1981.

Bouchon, M., The rupture mechanism of the Coyote Lake earthquake of 6 August 1979 inferred from near-field data, *Bull. Seism. Soc. Am., 72,* 745-757, 1982.

Courboulex, F., J. Virieux, A. Deschamps, D. Gibert, and A. Zollo, Source investigation of a small event using empirical Green's functions and simulated annealing, *Geophys. J. Int., 125,*, 768-780, 1996.

Ellsworth, W.L., and M. Celebi, Near field displacement time histories of the M 7.4 Kocaeli (Izmit), Turkey, earthquake of August 17, 1999, (abstract), *Eos trans. AGU, 80,* Fall Meeting supp., 648, 1999.

Hartzell, S., and P. Liu, Determination of earthquake source parameters using a hybrid global search algorithm, *Bull. Seism. Soc. Am., 85,* 516-524, 1995.

Ihmlé, P.F., Monte Carlo slip inversion in the frequency domain: Application to the 1992 Nicaragua slow earthquake, *Geophys. Res. Lett., 23,*, 913-916, 1996.

Toksöz, M.N., R.E. Reilinger, C.G. Doll, A.A. Barka, and N. Yalcin, Izmit (Turkey) earthquake of 17 August 1999: First Report, *Seism. Res. Lett., 70,* 669-679, 1999.

M. Bouchon and M. Dietrich, Laboratoire de Géophysique Interne et Tectonophysique, BP 53, 38041 Grenoble, France (e-mail: Michel.Bouchon@ujf-grenoble.fr)

N. Toksöz and M. Edie, Earth Resources Laboratory, MIT, 42 Carleton St., Cambridge MA 02142

H. Karabulut and M. Aktar, Kandilli Observatory, 81220 Çengelköy, Istanbul

M.P. Bouin, IPGP, 4 Place Jussieu, 75252 Paris

(Received May 8, 2000; revised June 28, 2000; accepted July 10, 2000.)